

SUPPRESSION OF RECURRENCE IN THE HERMITE-SPECTRAL METHOD FOR TRANSPORT EQUATIONS

ZHENNING CAI AND YANLI WANG

ABSTRACT. We study the unphysical recurrence phenomenon arising in the numerical simulation of the transport equations using Hermite-spectral method. From a mathematical point of view, the suppression of this numerical artifact with filters is theoretically analyzed for two types of transport equations. It is rigorously proven that all the non-constant modes are damped exponentially by the filters in both models, and formally shown that the filter does not affect the damping rate of the electric energy in the linear Landau damping problem. Numerical tests are performed to show the effect of the filters.

Keywords: Hermite spectral method; filter; recurrence

1. INTRODUCTION

We consider a system with a large number of microscopic particles, and the motion of these particles is governed by a force field. Instead of the state of every individual particle, we are interested in the collective behavior of these particles, such as the local density and the mean velocity. To obtain such information, the system needs to be properly modeled before carrying out the simulation. Compared with tracking the positions and velocities of all the particles as in the method of molecular dynamics, a more efficient method is to use the kinetic theory to describe the system in a statistical way. The basic idea of the kinetic theory is to introduce a velocity distribution function $f(\mathbf{x}, \boldsymbol{\xi}, t)$, which denotes the number density of particles in the position-velocity space, and the governing equation for f is

$$(1.1) \quad \frac{\partial f}{\partial t} + \boldsymbol{\xi} \cdot \nabla_{\mathbf{x}} f + \mathbf{E} \cdot \nabla_{\boldsymbol{\xi}} f = 0, \quad t \in \mathbb{R}^+, \quad \mathbf{x} \in \mathbb{R}^N, \quad \boldsymbol{\xi} \in \mathbb{R}^N,$$

where t denotes the time, \mathbf{x} denotes the position, and $\boldsymbol{\xi}$ stands for the velocity of the particles. The force field is given by \mathbf{E} . In this paper, we consider the one-dimensional case with periodic boundary condition in space, and thus the equation for $f(x, \xi, t)$ can be rewritten as

$$(1.2a) \quad \frac{\partial f}{\partial t} + \xi \frac{\partial f}{\partial x} + E \frac{\partial f}{\partial \xi} = 0, \quad t \in \mathbb{R}^+, \quad x \in \mathbb{R}, \quad \xi \in \mathbb{R},$$

$$(1.2b) \quad f(x, \xi, t) = f(x + D, \xi, t), \quad \forall (x, \xi, t) \in \mathbb{R} \times \mathbb{R} \times \mathbb{R}^+,$$

where D is the period, and we assume that E is also periodic and independent of the velocity ξ , but may be a function of t and x . A typical example of this model is the Vlasov-Poisson (VP) equation arising from the astrophysics and plasma physics, which models the system formed by a large number of charged particles, and the force is generated by a self-consistent electric field. Moreover, Landau damping is one of the fundamental problems in the applications of the VP equation. However, in the numerical simulations of Landau damping, it is observed that an unphysical phenomenon called ‘‘recurrence’’ occurs for most grid-based solvers [8].

This work is supported by National University of Singapore Startup Fund under Grant No. R-146-000-241-133. Yanli Wang is also supported by the National Natural Scientific Foundation of China (Grant No. 11501042) and China Scholarship Council.

The recurrence is an unphysical periodic behavior in the numerical solutions of the VP equation. It can be demonstrated by the simple advection equation ($E = 0$ in (1.2)) whose exact solution is $f(x, \xi, t) = f(x - \xi t, \xi, 0)$. It shows that any spatial wave in the initial condition will cause a wave in the velocity domain in the evolution of the solution, and the frequency of the wave gets higher when t increases. If the velocity domain is discretized by a fixed grid, the exact solution cannot be well resolved when t is large. Particularly, the numerical solution may look smoother than the exact solution and therefore appears similar to the solution at a previous time. Such phenomenon has been reported in a number of research works with different grid-based numerical methods [10, 26, 9, 28, 22]. The appearance of the recurrence may be postponed by using a larger number of velocity grids [30, 15], which also introduces larger computational cost. To avoid the recurrence, the particle-in-cell method [2, 18, 6] can be adopted and it is reported in [4] that the numerical result does not present recurrence. However, since the particle-in-cell method is a stochastic method, only half-order convergence can be achieved. An idea of combining the two types of methods is introduced in [1], where the authors suppress the recurrence by introducing some randomness into the grid-based methods.

In this paper, we consider another type of methods called transform methods [5, 13], where the distribution function is mapped to the frequency space and the Fourier modes are solved instead of the values on the grid points. Especially, we adopt the Hermite-spectral method introduced by [19] as the asymmetric Hermite method. The similar idea is adopted in [3] to get a slightly nonlinear discretization. For transform methods, one can suppress recurrence by introducing filters to the numerical methods [23, 7], or adding artificial collisions to the model [4, 24]. The suppression of the recurrence is numerically analyzed in [16], where it is shown that the collision has a damping effect for the high-frequency modes, so that the distribution function is smoothed out and the filamentation is weakened. However, a theoretical study of its underlying mathematical mechanism is still missing in the literature.

To fill the vacancy, we are going to conduct a theoretical analysis on the relation between the filters and the recurrence. The analysis is performed on two types of transport equations including the advection equation and Vlasov-Poisson equation. For both types of equations, it is shown by eigenvalue analysis that all the non-constant modes in the discrete system converge to zero exponentially as the time goes to infinity, and therefore the damping effect is rigorously proven. Moreover, it is formally shown that the filter does not change the damping rate of the electric energy in the case of linear Landau damping. Our numerical results are consistent with the analysis. In the tests for linear Landau damping, numerical results with high quality are observed with the filter introduced in [20].

The rest of this paper is organized as follows. In Section 2, we briefly introduce the Hermite-spectral method and the filters. In Section 3 and 4, two types of equations are analyzed respectively. Some numerical experiments are performed in Section 5, and the concluding remarks are given in Section 6.

2. HERMITE-SPECTRAL METHOD AND FILTERING

In this section, we focus on the velocity discretization of the Vlasov equation. Following [3], we consider the following approximation of the distribution function¹:

$$(2.1) \quad f(x, \xi, t) \approx \frac{1}{\sqrt{2\pi}} \sum_{i=0}^M f_i(x, t) He_i(\xi) \exp\left(-\frac{\xi^2}{2}\right),$$

¹In [3], the basis functions are translated and scaled in order to adapt the functions, while in this paper, such adaption is removed for easier analysis, and the resulting equations can be regarded as a linearized version of the model in [3].

where $He_i(\xi)$ is the normalized Hermite polynomials defined by

$$(2.2) \quad He_n(\xi) = \frac{(-1)^n}{\sqrt{n!}} \exp\left(\frac{\xi^2}{2}\right) \frac{d^n}{d\xi^n} \exp\left(-\frac{\xi^2}{2}\right),$$

and they have the following properties:

(1) Orthogonality:

$$(2.3) \quad \frac{1}{\sqrt{2\pi}} \int_{\mathbb{R}} He_m(\xi) He_n(\xi) \exp\left(-\frac{\xi^2}{2}\right) d\xi = \delta_{mn}, \quad \forall m, n \in \mathbb{N};$$

(2) Recursion relation:

$$(2.4) \quad \sqrt{n+1} He_{n+1}(\xi) = \xi He_n(\xi) - \sqrt{n} He_{n-1}(\xi), \quad \forall n \in \mathbb{N};$$

(3) Differential relation:

$$(2.5) \quad \begin{aligned} He'_{n+1}(\xi) &= \sqrt{n+1} He_n(\xi), \\ \frac{d}{d\xi} \left(He_n(\xi) \exp\left(-\frac{\xi^2}{2}\right) \right) &= -\sqrt{n+1} He_{n+1}(\xi) \exp\left(-\frac{\xi^2}{2}\right), \quad \forall n \in \mathbb{N}. \end{aligned}$$

Using these properties, the equations for the coefficients $f_i(x, t)$ can be derived by inserting (2.1) into (1.2) and integrating the result against $He_k(\xi)$ with $k = 0, \dots, M$. By defining $\mathbf{f} = (f_0, f_1, \dots, f_M)^T$, we have the following evolution equations:

$$(2.6) \quad \frac{\partial \mathbf{f}}{\partial t} + \mathbf{A} \frac{\partial \mathbf{f}}{\partial x} - \mathbf{E} \mathbf{B} \mathbf{f} = 0,$$

where \mathbf{A} and \mathbf{B} are $(M+1) \times (M+1)$ matrices defined by

$$(2.7) \quad \mathbf{A} = \begin{pmatrix} 0 & 1 & 0 & 0 & \dots & 0 \\ 1 & 0 & \sqrt{2} & 0 & \dots & 0 \\ 0 & \sqrt{2} & 0 & \sqrt{3} & \dots & 0 \\ 0 & \ddots & \ddots & \ddots & \ddots & \vdots \\ \vdots & \ddots & 0 & \sqrt{M-1} & 0 & \sqrt{M} \\ 0 & \dots & 0 & 0 & \sqrt{M} & 0 \end{pmatrix}, \quad \mathbf{B} = \begin{pmatrix} 0 & 0 & 0 & \dots & 0 \\ 1 & 0 & 0 & \dots & 0 \\ 0 & \sqrt{2} & 0 & \dots & 0 \\ \vdots & \ddots & \ddots & \ddots & \vdots \\ 0 & \dots & 0 & \sqrt{M} & 0 \end{pmatrix}.$$

The system (2.6) is the semi-discrete transport equation after spectral discretization of the velocity variable. As will be seen below, such discretization suffers from a deficiency called ‘‘recurrence phenomenon’’ [3, 23], which causes the non-physical echo of the electric energy when simulating the plasma. In [23], the authors proposed the filtered spectral method, and in the numerical results, the recurrence was clearly suppressed. Here we adopt the similar method and apply the filter after every time step. In detail, let $\mathbf{f}^n = (f_0^n, \dots, f_M^n)^T$ be the numerical solution of (2.6) at the n th time step, and suppose a numerical scheme for (2.6) is

$$(2.8) \quad \mathbf{f}^{n+1} = \mathbf{Q}(\mathbf{f}^n).$$

When a filter is applied, the above scheme is altered as

$$(2.9) \quad \begin{aligned} \mathbf{f}^{n,*} &= \mathbf{Q}(\mathbf{f}^n), \\ f_i^{n+1} &= \sigma_M(i) f_i^{n,*}, \quad i = 0, \dots, M, \end{aligned}$$

where the filter $\sigma_M(i)$ satisfies

$$(2.10) \quad \sigma_M(0) = 1, \quad \lim_{M \rightarrow \infty} \sigma_M(i) = 1, \quad \forall i \in \mathbb{N}.$$

The filter is often interpreted as an operator with the effect of diffusion [12]. Especially, when we take the exponential filter

$$(2.11) \quad \sigma_M(i) = \exp(-\alpha(i/M)^p),$$

the method (2.9) is actually computing the solution to the modified problem

$$(2.12) \quad \frac{\partial f}{\partial t} + \xi \frac{\partial f}{\partial x} + E \frac{\partial f}{\partial \xi} = -\alpha \frac{(-1)^p}{\Delta t M^p} \mathcal{D}^p f,$$

where \mathcal{D} is a linear operator defined by

$$(2.13) \quad \mathcal{D}f(x, \xi, t) = \frac{\partial}{\partial \xi} \left[\exp\left(-\frac{\xi^2}{2}\right) \frac{\partial}{\partial \xi} \left(\exp\left(\frac{\xi^2}{2}\right) f(x, \xi, t) \right) \right].$$

The time step Δt needs to be chosen to ensure stability. Since $\|\mathbf{B}\|_2 = \sqrt{M}$ and the maximum eigenvalue of \mathbf{A} is the maximum zero of $He_{M+1}(\xi)$, which grows asymptotically as $O(\sqrt{M})$, we choose the time step as $\Delta t \sim O(M^{-1/2})$ in this work. Thus one sees that when M gets larger, the equation formally converges to the transport equation (1.2) if $p > 1/2$.

When the original transport equation (1.2) is replaced by (2.12), the semi-discrete system (2.6) changes to

$$(2.14) \quad \frac{\partial \mathbf{f}}{\partial t} + \mathbf{A} \frac{\partial \mathbf{f}}{\partial x} - E \mathbf{B} \mathbf{f} = \mathbf{H} \mathbf{f},$$

where $\mathbf{H} = -\Delta t^{-1} \alpha \text{diag}\{0, (1/M)^p, \dots, [(M-1)/M]^p, 1\}$. In general, we assume that

$$(2.15) \quad \mathbf{H} = \text{diag}\{h_0, h_1, \dots, h_M\}$$

is an $(M+1)$ by $(M+1)$ diagonal matrix with non-positive diagonal entries, and in order to keep the conservation of total number of particles, we require that the first entry $h_0 = 0$.

Below we are going to remove the spatial derivative by Fourier series expansion. The periodic boundary condition (1.2b) shows that \mathbf{f} is also periodic with respect to x . Thus we have the following series expansions:

$$(2.16) \quad \mathbf{f} = \sum_{m \in \mathbb{Z}} \hat{\mathbf{f}}^{(m)} \exp(imkx), \quad E = \sum_{m \in \mathbb{Z}} \hat{E}^{(m)} \exp(imkx), \quad k = 2\pi/D,$$

and Parseval's equality shows that

$$(2.17) \quad \|\mathbf{f}\|_2^2 = D \sum_{m \in \mathbb{Z}} \left\| \hat{\mathbf{f}}^{(m)} \right\|_2^2, \quad \|E\|_2^2 = D \sum_{m \in \mathbb{Z}} |\hat{E}^{(m)}|^2.$$

Substituting (2.16) into (2.14), we get the equations for the Fourier coefficients $\hat{\mathbf{f}}^{(m)}$:

$$(2.18) \quad \frac{\partial \hat{\mathbf{f}}^{(m)}}{\partial t} + imk \mathbf{A} \hat{\mathbf{f}}^{(m)} - \sum_{l \in \mathbb{Z}} \hat{E}^{(l)} \mathbf{B} \hat{\mathbf{f}}^{(m-l)} = \mathbf{H} \hat{\mathbf{f}}^{(m)}, \quad m \in \mathbb{Z}.$$

Based on the form (2.18), we will show in the following sections that the filter \mathbf{H} can suppress the recurrence phenomenon, especially in the simulation of Landau damping.

3. ADVECTION EQUATION

3.1. Recurrence without filter. We will begin our discussion with a simple case $E = 0$, and thus the transport equation (1.2) becomes

$$(3.1) \quad \frac{\partial f}{\partial t} + \xi \frac{\partial f}{\partial x} = 0, \quad t \in \mathbb{R}^+, \quad x \in \mathbb{D}, \quad \xi \in \mathbb{R},$$

where $\mathbb{D} = [0, D]$ and the periodic boundary condition is imposed. It is known that the recurrence can be observed in such a simple advection equation with initial value

$$(3.2) \quad f(x, \xi, 0) = \frac{1}{\sqrt{2\pi}}(1 + \epsilon \cos(kx)) \exp\left(-\frac{\xi^2}{2}\right), \quad k = \frac{2\pi}{D},$$

and the recurrence time can be exactly given if the velocity is discretized with a uniform grid [25, 1]. For Hermite-spectral method, the system (2.18) is correspondingly reduced to

$$(3.3) \quad \frac{\partial \hat{\mathbf{f}}^{(m)}}{\partial t} + imk\mathbf{A}\hat{\mathbf{f}}^{(m)} = \mathbf{H}\hat{\mathbf{f}}^{(m)}, \quad m \in \mathbb{Z}.$$

If no filter is applied, $\mathbf{H} = 0$, and then the solution to the above system is

$$(3.4) \quad \hat{\mathbf{f}}^{(m)}(t) = \exp(-imkt\mathbf{A})\hat{\mathbf{f}}^{(m)}(0) = \mathbf{R}^T \exp(-imkt\mathbf{\Lambda}) \mathbf{R}\hat{\mathbf{f}}^{(m)}(0),$$

where \mathbf{R} is an $(M+1) \times (M+1)$ orthogonal matrix satisfying $\mathbf{R}\mathbf{\Lambda}\mathbf{R}^T = \mathbf{A}$, and $\mathbf{\Lambda}$ is an $(M+1) \times (M+1)$ real diagonal matrix due to the symmetry of the real matrix \mathbf{A} . The equality (3.4) indicates that

$$(3.5) \quad \|\hat{\mathbf{f}}^{(m)}(t)\|_2^2 = \|\hat{\mathbf{f}}^{(m)}(0)\|_2^2, \quad \forall m \in \mathbb{Z}, \quad t \in \mathbb{R}^+.$$

To observe the recurrence, we suppose that the exact solution to (3.1) and (3.2) can be written as

$$(3.6) \quad f(x, \xi, t) = \frac{1}{\sqrt{2\pi}} \sum_{i=0}^M \sum_{m \in \mathbb{Z}} \hat{f}_{\text{ex},i}^{(m)}(t) \exp(imkx) He_i(\xi) \exp\left(-\frac{\xi^2}{2}\right).$$

By straightforward calculation, we have

$$(3.7) \quad \hat{f}_{\text{ex},i}^{(m)}(t) = \begin{cases} \delta_{i0}, & \text{if } m = 0, \\ \frac{\epsilon}{2} \frac{(imkt)^i}{\sqrt{i!}} \exp\left(-\frac{k^2 t^2}{2}\right), & \text{if } m = \pm 1, \\ 0, & \text{otherwise.} \end{cases}$$

Therefore

$$(3.8) \quad \sum_{i=0}^M |\hat{f}_{\text{ex},i}^{(\pm 1)}(t)|^2 = \frac{\epsilon^2}{4} \sum_{i=0}^M \frac{(kt)^{2i}}{i!} \exp(-k^2 t^2),$$

which decays to zero as $t \rightarrow \infty$. The relation (3.5) shows that this property is not maintained after discretization. In fact, if $(2\pi)^{-1}kt\mathbf{\Lambda}$ is close to an integer matrix for some t , then $\hat{\mathbf{f}}^{(m)}(t)$ is close to $\hat{\mathbf{f}}^{(m)}(0)$ for all $m \in \mathbb{Z}$, which turns out to be a ‘‘recurrence’’. Some illustration will be given in Section 5.

3.2. Suppression of recurrence with filter. When a filter is applied, the solution to (3.3) is

$$(3.9) \quad \hat{\mathbf{f}}^{(m)}(t) = \exp\left((-imk\mathbf{A} + \mathbf{H})t\right)\hat{\mathbf{f}}^{(m)}(0).$$

In this subsection, we assume that \mathbf{H} is a filter whose first diagonal entry is zero and last diagonal entry is nonzero. Actually, almost all filters have such a form so that the high-frequency modes can be damped while the low-frequency modes are not disturbed. Based on this assumption, we have the following theorem:

Theorem 1. *Let $\mathbf{A}_m = -imk\mathbf{A} + \mathbf{H}$. Then for all $m \in \mathbb{Z} \setminus \{0\}$, all the eigenvalues of \mathbf{A}_m have negative real parts.*

The above theorem shows that for all $m \in \mathbb{Z} \setminus \{0\}$, $\hat{\mathbf{f}}^{(m)}(t) \rightarrow 0$ as $t \rightarrow +\infty$, which fixes the undesired property (3.5), and agrees with the decaying behavior of the exact solution to the advection equation. Thus the recurrence is suppressed. The proof of the theorem requires the following lemma:

Lemma 1. *Let $\mathbf{M} = (a_{ij})_{N \times N}$ be a symmetric tridiagonal matrix with nonzero subdiagonal entries. Define $p_n(\lambda)$, $n = 1, \dots, N$ as the characteristic polynomial of the n th order leading principle submatrix of \mathbf{M} . Then the following statements hold:*

- *The roots of p_n and p_{n+1} are interlacing;*
- *If λ is an eigenvalue of \mathbf{M} , then the associated eigenvector is $\mathbf{r} = (r_1, \dots, r_N)^T$ with $r_1 = 1$ and $r_n = (-1)^{n-1} p_{n-1}(\lambda) / (a_{12} a_{23} \cdots a_{n-1,n})$ for $n > 1$;*
- *If $\mathbf{r} = (r_1, \dots, r_N)^T$ is an eigenvector of \mathbf{M} , then $r_N \neq 0$.*

In the above lemma, the first statement is a well-known result for the interlacing system. We refer the readers to [14] for the proof. The second result can be found in [29] and it can also be checked directly using the definition of eigenvectors. The third statement is obviously a result of the first two statements.

Now we give the proof of Theorem 1 as below:

Proof of Theorem 1. Let λ be an eigenvalue of \mathbf{A}_m for some $m \in \mathbb{Z} \setminus \{0\}$. We first show that $\text{Re } \lambda \leq 0$. Suppose \mathbf{r} is the associated eigenvector. Using $\mathbf{A}_m \mathbf{r} = \lambda \mathbf{r}$, we have that

$$(3.10) \quad 0 \geq 2\mathbf{r}^* \mathbf{H} \mathbf{r} = \mathbf{r}^* (\mathbf{A}_m^* + \mathbf{A}_m) \mathbf{r} = (\lambda + \bar{\lambda}) \mathbf{r}^* \mathbf{r} = 2\|\mathbf{r}\|^2 \text{Re } \lambda.$$

Thus $\text{Re } \lambda \leq 0$.

It remains only to show that $\text{Re } \lambda \neq 0$. If there exist $\lambda_I \in \mathbb{R}$ and $\mathbf{r} \in \mathbb{C}^{M+1}$, such that $\mathbf{A}_m \mathbf{r} = i\lambda_I \mathbf{r}$, then

$$(3.11) \quad i\lambda_I \|\mathbf{r}\|^2 = \mathbf{r}^* \mathbf{A}_m \mathbf{r} = -imk \mathbf{r}^* \mathbf{A} \mathbf{r} + \mathbf{r}^* \mathbf{H} \mathbf{r}.$$

The symmetry of both \mathbf{A} and \mathbf{H} yields $\mathbf{r}^* \mathbf{H} \mathbf{r} = 0$, which is equivalent to $\mathbf{H} \mathbf{r} = 0$ since \mathbf{H} is diagonal. Recalling that the last diagonal entry of \mathbf{H} is assumed to be strictly negative, we know that the last component of \mathbf{r} is zero. Furthermore, we have

$$(3.12) \quad \mathbf{A} \mathbf{r} = \frac{i}{mk} (\mathbf{A}_m - \mathbf{H}) \mathbf{r} = -\frac{\lambda_I}{mk} \mathbf{r},$$

which indicates that \mathbf{r} is an eigenvector of \mathbf{A} . According to Lemma 1, the last component of \mathbf{r} must be nonzero, which is a contradiction. Therefore \mathbf{A}_m does not have purely imaginary eigenvalues, which concludes the proof. \square

The following theorem shows that the convergence rate has a lower bound for all non-constant Fourier modes:

Theorem 2. *For all $m \in \mathbb{Z} \setminus \{0\}$, suppose*

$$(3.13) \quad \mathbf{A}_m := -imk \mathbf{A} + \mathbf{H} = \mathbf{R}_m \mathbf{J}_m \mathbf{R}_m^{-1},$$

where \mathbf{J}_m is the Jordan normal form of \mathbf{A}_m , and every column of \mathbf{R}_m is a unit vector. Then there exists a constant $C^{(0)} > 0$, such that

$$(3.14) \quad \|\mathbf{R}_m\|_2 \leq C^{(0)}, \quad \|\mathbf{R}_m^{-1}\|_2 \leq C^{(0)}.$$

And there exists a constant $\lambda^{(0)} > 0$, such that for any $m \in \mathbb{Z} \setminus \{0\}$, all the eigenvalues of \mathbf{A}_m have real parts less than $-\lambda^{(0)}$.

Proof. Consider the matrix

$$(3.15) \quad \mathbf{B}_m := \frac{i}{mk} \mathbf{A}_m = \mathbf{A} + \frac{i}{mk} \mathbf{H}, \quad m \in \mathbb{Z} \setminus \{0\}.$$

Apparently the characteristic polynomial of \mathbf{B}_m converges to the characteristic polynomial of \mathbf{A} as $m \rightarrow \infty$. Thus all the eigenvalues of \mathbf{B}_m also converge to the eigenvalues of \mathbf{A} as $m \rightarrow \infty$. Lemma 1 implies that all the eigenvalues of \mathbf{A} are distinct. Therefore there exists an $m_0 > 0$ such that all the eigenvalues of \mathbf{B}_m are distinct if $|m| > m_0$. The relation between \mathbf{A}_m and \mathbf{B}_m indicates that all the eigenvalues of \mathbf{A}_m are also distinct when $|m| > m_0$. In this case, the similarity transformation (3.13) becomes a diagonalization of \mathbf{A}_m , and every column of \mathbf{R}_m is a unit eigenvector of \mathbf{A}_m (or \mathbf{B}_m).

To show the bound (3.14), it is sufficient to show that $\|\mathbf{R}_m\|_2$ and $\|\mathbf{R}_m^{-1}\|_2$ have a uniform upper bound for all $|m| > m_0$. Let $\mathbf{r}_i^{(m)}$ be the i th column of \mathbf{R}_m , and suppose $\mathbf{B}_m \mathbf{r}_i^{(m)} = \mu_i^{(m)} \mathbf{r}_i^{(m)}$. Since exchanging two columns of \mathbf{R}_m does not change the norms $\|\mathbf{R}_m\|_2$ and $\|\mathbf{R}_m^{-1}\|_2$, we can assume

$$(3.16) \quad \lim_{m \rightarrow \infty} \mu_i^{(m)} = \lambda_i,$$

where λ_i is the i th eigenvalue of \mathbf{A} . Using the fact that $\mathbf{r}_i^{(m)}$ is a unit vector, we have that

$$0 = \lim_{m \rightarrow \infty} \left(\mathbf{B}_m - \mu_i^{(m)} \mathbf{I} \right) \mathbf{r}_i^{(m)} = \lim_{m \rightarrow \infty} \left(\mathbf{A} - \lambda_i \mathbf{I} \right) \mathbf{r}_i^{(m)}.$$

Hence,

$$(3.17) \quad \lim_{m \rightarrow \infty} \mathbf{r}_i^{(m)} = \mathbf{r}_i,$$

where \mathbf{r}_i is the unit eigenvector of \mathbf{A} associated with the eigenvalue λ_i . Thus \mathbf{R}_m has a limit \mathbf{R} as $m \rightarrow \infty$, and the limit diagonalizes \mathbf{A} as $\mathbf{A} = \mathbf{R} \mathbf{\Lambda} \mathbf{R}^{-1}$, which naturally leads to the bound (3.14).

To show that the bound $\lambda^{(0)}$ exists, we use the unity of vectors $\mathbf{r}_i^{(m)}$ to get

$$(3.18) \quad \lim_{m \rightarrow \infty} \operatorname{Re} \lambda_i^{(m)} = \lim_{m \rightarrow \infty} \operatorname{Re} \left(\left(\mathbf{r}_i^{(m)} \right)^* \mathbf{A}_m \mathbf{r}_i^{(m)} \right) = \lim_{m \rightarrow \infty} \left(\mathbf{r}_i^{(m)} \right)^* \mathbf{H} \mathbf{r}_i^{(m)} = \mathbf{r}_i^* \mathbf{H} \mathbf{r}_i < 0.$$

The last inequality comes from the proof of Theorem 1. The existence of the negative limit shows the existence of the negative upper bound. \square

The above theorem gives an upper bound for the real parts of the eigenvalues. A direct corollary is

Corollary 1. $\forall m \in \mathbb{Z}$ and $t > 0$, $\|\exp(t\mathbf{A}_m)\|_2$ is uniformly bounded, and if $m \neq 0$, it holds that

$$(3.19) \quad \|\exp(t\mathbf{A}_m)\|_2 \leq C^{(1)} (t^M + 1) \exp\left(-\lambda^{(0)}t\right),$$

where $C^{(1)} = (M+1)(C^{(0)})^2$, and the constants $\lambda^{(0)}$ and $C^{(0)}$ are introduced in Theorem 2.

The estimate (3.19) is a result of Theorem 2 and the following lemma:

Lemma 2. For any matrix \mathbf{M} , suppose \mathbf{J} is its Jordan normal form and $\mathbf{M} = \mathbf{X} \mathbf{J} \mathbf{X}^{-1}$. The following estimate holds for the norm of $\exp(t\mathbf{M})$:

$$(3.20) \quad \|\exp(t\mathbf{M})\|_2 \leq \beta \|\mathbf{X}\|_2 \|\mathbf{X}^{-1}\|_2 \max_{0 \leq i \leq \beta-1} \frac{t^i}{i!} e^{-\alpha t},$$

where β is the maximum dimension of the Jordan blocks, and α is the maximum real part of the eigenvalues of \mathbf{M} .

The lemma can be found in [21]. The uniform boundedness in Corollary 1 is an immediate result of (3.19) and $\|\exp(t\mathbf{A}_0)\|_2 = \|\exp(t\mathbf{H})\|_2 = 1$.

The estimate (3.19) shows the linearly exponential decay of the non-constant Fourier modes. Compared with (3.8), the decay rate is still not fast enough, which indicates that the recurrence is not fully removed. However, when M is sufficiently large, the filtered spectral method can give accurate approximation of the decay rate up to some time T , and after time T , the values of both the exact solution and the numerical solution are already small enough, and therefore the numerical result can still be considered as accurate, although the decay rate may not be exact. Examples will be given in Section 5 to show the aforementioned behavior.

3.3. Advection Equation with an Exponentially Decaying Force. The above result can be extended to the case with a given decaying force field. Here we assume that

$$(3.21) \quad E(x, t) = \exp(-\alpha(t))w(x, t), \quad x \in \mathbb{D},$$

where $\alpha(t) \geq \alpha_E t > 0$ and $w(x, t) \in L^\infty(\mathbb{D} \times [0, +\infty))$. Such a force field mimics the electric force field in the Vlasov-Poisson equations, where the self-consistent force decays exponentially. Therefore, it can be expected that the behavior of this equation is similar to the linear Landau damping. Again, we study the equations of Fourier coefficients (2.18) instead of the original system (2.14). It will be shown that the system (2.14) has a steady state solution in which only the constant modes are nonzero. Here we only consider the case with filter, which means that the last diagonal entry of \mathbf{H} is strictly negative.

For the purely advective equation, each $\hat{\mathbf{f}}^{(m)}$ can be considered independently, while in this case, the Fourier coefficients $\hat{\mathbf{f}}^{(m)}$ are fully coupled for all $m \in \mathbb{Z}$. Therefore, we define a Hilbert space \mathcal{H} whose elements have the form

$$(3.22) \quad \hat{\mathbf{g}} = \left(\dots, \hat{\mathbf{g}}^{(-m)}, \dots, \hat{\mathbf{g}}^{(-1)}, \hat{\mathbf{g}}^{(0)}, \hat{\mathbf{g}}^{(1)}, \dots, \hat{\mathbf{g}}^{(m)}, \dots \right),$$

where each $\hat{\mathbf{g}}^{(m)}$ is a vector in \mathbb{C}^{M+1} . For any vector in \mathcal{H} , below we always use the superscript “ (m) ” to denote its m th component as in (3.22). The inner product of \mathcal{H} is defined as

$$(3.23) \quad \langle \hat{\mathbf{g}}_1, \hat{\mathbf{g}}_2 \rangle = \sum_{m \in \mathbb{Z}} (\hat{\mathbf{g}}_1^{(m)})^* \hat{\mathbf{g}}_2^{(m)}, \quad \forall \hat{\mathbf{g}}_1, \hat{\mathbf{g}}_2 \in \mathcal{H}.$$

Therefore by Parseval’s inequality (2.17), \mathcal{H} corresponds to the space $[L^2(\mathbb{D})]^{M+1}$ in the original space. For the purpose of uniformity, the norm in the Hilbert space \mathcal{H} is denoted as $\|\cdot\|_2$ below.

To represent the system (2.14), we introduce two operators $\hat{\mathbf{A}}$ and $\hat{\mathbf{B}}(t)$, which are transformations on \mathcal{H} , defined by

$$(3.24) \quad \begin{aligned} \tilde{\mathbf{g}} &= \hat{\mathbf{A}}\mathbf{g} \iff \tilde{\mathbf{g}}^{(m)} = \mathbf{A}_m \mathbf{g}^{(m)}, \quad \forall m \in \mathbb{Z}, \\ \tilde{\mathbf{g}} &= \hat{\mathbf{B}}(t)\mathbf{g} \iff \tilde{\mathbf{g}}^{(m)} = \sum_{l \in \mathbb{Z}} \hat{w}^{(l)}(t) \mathbf{B} \mathbf{g}^{(m-l)}, \quad \forall m \in \mathbb{Z}. \end{aligned}$$

where the matrix \mathbf{A}_m is defined in Theorem 1 as $\mathbf{A}_m = -imk\mathbf{A} + \mathbf{H}$, and $\hat{w}^{(l)}(t)$ are the Fourier coefficients for $w(x, t)$:

$$(3.25) \quad w(x, t) = \sum_{m \in \mathbb{Z}} \hat{w}^{(m)}(t) \exp(ikx), \quad m \in \mathbb{Z}.$$

Thus (2.14) can be written as

$$(3.26) \quad \frac{\partial \hat{\mathbf{f}}(t)}{\partial t} = \hat{\mathbf{A}} \hat{\mathbf{f}}(t) + \exp(-\alpha(t)) \hat{\mathbf{B}}(t) \hat{\mathbf{f}}(t).$$

Here $\hat{\mathbf{f}}(\cdot)$ is a map from \mathbb{R}^+ to \mathcal{H} . Applying Duhamel's principle, we can obtain its integral form as

$$(3.27) \quad \hat{\mathbf{f}}(t) = \exp\left(t\hat{\mathbf{A}}\right) \hat{\mathbf{f}}(0) + \int_0^t \exp(-\alpha(s)) \exp\left((t-s)\hat{\mathbf{A}}\right) \hat{\mathbf{B}}(s) \hat{\mathbf{f}}(s) ds.$$

For the operators $\exp(t\hat{\mathbf{A}})$ and $\hat{\mathbf{B}}(t)$, we claim that

Lemma 3. *For all $t \geq 0$, the operators $\exp(t\hat{\mathbf{A}})$ and $\hat{\mathbf{B}}(t)$ are uniformly bounded, i.e. there exist constants C_A and C_B such that*

$$(3.28) \quad \left\| \exp(t\hat{\mathbf{A}}) \right\|_2 \leq C_A, \quad \left\| \hat{\mathbf{B}}(t) \right\|_2 \leq C_B, \quad \forall t > 0.$$

This lemma can be easily obtained by Corollary 1 and the boundedness of $w(x, t)$. The detailed proof is left for the readers. Below we state the main result of this subsection:

Theorem 3. *Let $\hat{\mathbf{f}}(t)$ be the solution to (3.27). There exists $\hat{\mathbf{f}}_\infty \in \mathcal{H}$ such that*

$$(3.29) \quad \lim_{t \rightarrow +\infty} \left\| \hat{\mathbf{f}}(t) - \hat{\mathbf{f}}_\infty \right\|_2 = 0,$$

and $\hat{\mathbf{f}}_\infty$ satisfies

$$(3.30) \quad \hat{\mathbf{f}}_\infty^{(m)} = 0, \quad \forall m \in \mathbb{Z} \setminus \{0\}.$$

This theorem shows that the steady solution of (2.14) exists and is a constant. It is known from Section 3.1 that when recurrence appears, some non-constant modes will never decay, which causes the phenomenon that similar solutions appear again and again when all these modes are close to the peaks of the waves. Consequently, no steady state solution exists in such a case. In this sense, the theorem implies the suppression of recurrence by the filter. Before proving this theorem, we first show the boundedness of the solution:

Lemma 4. *Let $\hat{\mathbf{f}}$ be the solution to (3.27). Then there exists a constant C_f such that*

$$(3.31) \quad \left\| \hat{\mathbf{f}}(t) \right\|_2 \leq C_f \left\| \hat{\mathbf{f}}(0) \right\|_2.$$

Proof. Taking the norm on both sides of (3.27) and plugging in the inequalities (3.28), we obtain

$$(3.32) \quad \begin{aligned} \left\| \hat{\mathbf{f}}(t) \right\|_2 &\leq C_A \left\| \hat{\mathbf{f}}(0) \right\|_2 + C_A \int_0^t \exp(-\alpha(s)) \left\| \hat{\mathbf{B}} \hat{\mathbf{f}}(s) \right\|_2 ds \\ &\leq C_A \left\| \hat{\mathbf{f}}(0) \right\|_2 + C_A C_B \int_0^t \exp(-\alpha_E s) \left\| \hat{\mathbf{f}}(s) \right\|_2 ds \end{aligned}$$

By Gronwall's inequality, we immediately have the estimation (3.31) with the constant $C_f = C_A \exp(\|w\|_\infty C_A C_B / \alpha_E)$. \square

Now we present the proof of Theorem 3:

Proof of Theorem 3. Let $\hat{\mathbf{b}}(t) = \hat{\mathbf{B}}(t) \hat{\mathbf{f}}(t)$. The boundedness of $\hat{\mathbf{B}}(t)$ and Lemma 4 yield that

$$(3.33) \quad \left\| \hat{\mathbf{b}}(t) \right\|_2 \leq C_B C_f \left\| \hat{\mathbf{f}}(0) \right\|_2.$$

Writing the integral system (3.27) as

$$(3.34) \quad \hat{\mathbf{f}}^{(m)}(t) = \exp(t\mathbf{A}_m) \hat{\mathbf{f}}^{(m)}(0) + \int_0^t \exp(-\alpha(s)) \exp((t-s)\mathbf{A}_m) \hat{\mathbf{b}}^{(m)}(s) ds, \quad \forall m \in \mathbb{Z},$$

we can bound $\|\hat{\mathbf{f}}^{(m)}(t)\|_2$ with $m \in \mathbb{Z} \setminus \{0\}$ by

$$\begin{aligned}
(3.35) \quad & \left(\sum_{m \in \mathbb{Z} \setminus \{0\}} \|\hat{\mathbf{f}}^{(m)}(t)\|_2^2 \right)^{1/2} \leq C^{(1)}(t^M + 1) \exp(-\lambda^{(0)}t) \left(\sum_{m \in \mathbb{Z} \setminus \{0\}} \|\hat{\mathbf{f}}^{(m)}(0)\|_2^2 \right)^{1/2} \\
& + \int_0^t C^{(1)}[(t-s)^M + 1] \exp(-\lambda^{(0)}(t-s)) \exp(-\alpha_E s) \left(\sum_{m \in \mathbb{Z} \setminus \{0\}} \|\hat{\mathbf{b}}^{(m)}(s)\|_2^2 \right)^{1/2} ds \\
& \leq C^{(1)}(t^M + 1) \exp(-\lambda^{(0)}t) \left(\|\hat{\mathbf{f}}(0)\|_2 + \int_0^t \exp((\lambda^{(0)} - \alpha_E)s) \|\hat{\mathbf{b}}(s)\|_2 ds \right) \\
& \leq C^{(1)}(t^M + 1) \left(\exp(-\lambda^{(0)}t) + \frac{C_B C_f}{|\lambda^{(0)} - \alpha_E|} [\exp(-\lambda^{(0)}t) + \exp(-\alpha_E t)] \right).
\end{aligned}$$

The right hand side goes to zero as t goes to infinity. Thus it remains only to prove $\hat{\mathbf{f}}^{(0)}(t)$ has a limit.

When $m = 0$, the equation (3.34) becomes

$$(3.36) \quad \hat{\mathbf{f}}^{(0)}(t) = \exp(t\mathbf{H})\hat{\mathbf{f}}^{(0)}(0) + \int_0^t \exp(-\alpha(s)) \exp((t-s)\mathbf{H})\hat{\mathbf{b}}^{(0)}(s) ds.$$

For any $i = 0, \dots, M$, if $h_i < 0$, we can still get $\hat{f}_i^{(0)}(+\infty) = 0$ using the same method as in (3.35). If $h_i = 0$,

$$(3.37) \quad \lim_{t \rightarrow +\infty} \hat{f}_i^{(0)}(t) = \hat{f}_i^{(0)}(0) + \int_0^{+\infty} \exp(-\alpha(s)) \hat{b}_i^{(0)}(s) ds.$$

The uniform boundedness of $\hat{b}_i^{(0)}$ and $\alpha(t) \geq \alpha_E t > 0$ shows the convergence of the integral on the right hand side, which concludes the proof. \square

Remark 1. In Theorem 3, one can also observe an exponential convergence rate to the steady state solution. However, the convergence rate depends on both the eigenvalue bound $\lambda^{(0)}$ and the decay rate of the force field α_E , whereas in Section 3.2, the convergence rates depend only on the eigenvalue bounds. In fact, if the force field does not decay, the steady state solution may not exist. A simple example is to let E be a constant. Then the distribution function will keep moving in the velocity space, and there is no mechanism which balances such a force to achieve the steady state. It can also be expected that current velocity discretization cannot well describe the system when t is large.

4. LINEAR LANDAU DAMPING IN THE VLASOV-POISSON EQUATION

In this section, we will generalize the result to the linear Landau damping problem, for which the recurrence in the electric energy has been widely observed [24, 10]. To study the linear Landau damping, we consider the dimensionless Vlasov-Poisson (VP) equation which models the motion of a collection of charged particles in the self-consistent electric field. For a given distribution function $f(x, \xi, t)$, the self-consistent electric field $E_{sc}(x, t)$ is given by

$$(4.1) \quad \frac{\partial E_{sc}(x, t)}{\partial x} = \left(\int_{\mathbb{R}} f(x, \xi, t) d\xi - \frac{1}{D} \int_{\mathbb{D} \times \mathbb{R}} f(x, \xi, t) d\xi dx \right).$$

with constraint

$$(4.2) \quad \int_{\mathbb{D}} E_{sc}(x, t) dx = 0.$$

Thus the Vlasov-Poisson equation can be written as (1.2) with $E(x, t) = E_{\text{sc}}(x, t)$. The initial condition is a uniform Gaussian distribution with perturbed electric charge density in the x -space:

$$(4.3) \quad f(x, \xi, 0) = \frac{1}{\sqrt{2\pi}} [1 + \epsilon \exp(ikx)] \exp\left(-\frac{\xi^2}{2}\right).$$

When ϵ is small, it is known that the total electric energy

$$(4.4) \quad \mathcal{E}(t) = \sqrt{\int_{\mathbb{D}} |E_{\text{sc}}(x, t)|^2 dx}$$

decays exponentially. For this example, we say that a recurrence exists in some numerical methods if the electric energy does not decay with time.

4.1. Asymptotic expansion and recurrence. Following the classical analysis [11], we expand the coefficients $\mathbf{f} = (f_0, f_1, \dots, f_M)^T$ in terms of ϵ :

$$(4.5) \quad \mathbf{f}(x, t) = \hat{\mathbf{f}}^{(0)}(t) + \epsilon \hat{\mathbf{f}}^{(1)}(t) \exp(ikx) + \epsilon^2 \hat{\mathbf{f}}^{(2)}(t) \exp(2ikx) + \dots,$$

where $\hat{\mathbf{f}}^{(m)} = (\hat{f}_0^{(m)}, \hat{f}_1^{(m)}, \dots, \hat{f}_M^{(m)})^T$. Correspondingly, the electric field $E(x, t)$ is expanded as

$$(4.6) \quad E(x, t) = \epsilon \hat{E}^{(1)}(t) \exp(ikx) + \epsilon^2 \hat{E}^{(2)}(t) \exp(2ikx) + \epsilon^3 \hat{E}^{(3)}(t) \exp(3ikx) + \dots.$$

Note that the definitions of $\hat{\mathbf{f}}^{(m)}$ and $\hat{E}^{(m)}$ are slightly different from those defined in (2.16). In this section, these symbols denote the Fourier coefficients scaled by ϵ^m . Inserting (4.5)(4.6) and (2.1) into (4.1), we get that

$$(4.7) \quad \hat{E}^{(m)} = -\frac{i}{mk} \hat{f}_0^{(m)}, \quad \forall m = 1, 2, \dots.$$

The equations for the coefficients of all orders can be obtained by substituting (4.5) and (4.6) into (2.14) and matching the terms with the same orders of ϵ :

$$O(1): \quad \frac{\partial \hat{\mathbf{f}}^{(0)}}{\partial t} = \mathbf{H} \hat{\mathbf{f}}^{(0)}, \quad \hat{\mathbf{f}}^{(0)}(0) = (1, 0, \dots, 0)^T.$$

$$O(\epsilon): \quad \frac{\partial \hat{\mathbf{f}}^{(1)}}{\partial t} + ik \mathbf{A} \hat{\mathbf{f}}^{(1)} + \frac{i}{k} \hat{f}_0^{(1)} \mathbf{B} \hat{\mathbf{f}}^{(0)} = \mathbf{H} \hat{\mathbf{f}}^{(1)}, \quad \hat{\mathbf{f}}^{(1)}(0) = (1, 0, \dots, 0)^T.$$

$$O(\epsilon^m): \quad \frac{\partial \hat{\mathbf{f}}^{(m)}}{\partial t} + imk \mathbf{A} \hat{\mathbf{f}}^{(m)} + \frac{i}{mk} \hat{f}_0^{(m)} \mathbf{B} \hat{\mathbf{f}}^{(0)} + \frac{i}{k} \sum_{l=1}^{m-1} \frac{1}{l} \hat{f}_0^{(l)} \mathbf{B} \hat{\mathbf{f}}^{(m-l)} = \mathbf{H} \hat{\mathbf{f}}^{(m)}, \quad \hat{\mathbf{f}}^{(m)}(0) = 0.$$

The last equation holds for all $m \geq 2$. Recalling that \mathbf{H} is a diagonal matrix with its first entry being zero, we can easily obtain from the $O(1)$ equation that $\hat{\mathbf{f}}^{(0)}(t) \equiv \hat{\mathbf{f}}^{(0)}(0) = (1, 0, \dots, 0)^T$. Therefore the other two equations can be rewritten as

$$(4.8) \quad \frac{\partial \hat{\mathbf{f}}^{(1)}}{\partial t} + ik \left(\mathbf{A} + \frac{1}{k^2} \mathbf{G} \right) \hat{\mathbf{f}}^{(1)} = \mathbf{H} \hat{\mathbf{f}}^{(1)}, \quad \hat{\mathbf{f}}^{(1)}(0) = (1, 0, \dots, 0)^T;$$

$$(4.9) \quad \frac{\partial \hat{\mathbf{f}}^{(m)}}{\partial t} + imk \left(\mathbf{A} + \frac{1}{(mk)^2} \mathbf{G} \right) \hat{\mathbf{f}}^{(m)} + \frac{i}{k} \sum_{l=1}^{m-1} \hat{f}_0^{(l)} \mathbf{B} \hat{\mathbf{f}}^{(m-l)} = \mathbf{H} \hat{\mathbf{f}}^{(m)}, \quad \hat{\mathbf{f}}^{(m)}(0) = 0.$$

Here we have used the symbol \mathbf{G} to denote the $(M+1) \times (M+1)$ matrix with only one nonzero entry locating at the second row and first column:

$$(4.10) \quad \mathbf{G} = \begin{pmatrix} 0 & 0 & \cdots & 0 \\ 1 & 0 & \cdots & 0 \\ 0 & 0 & \cdots & 0 \\ \vdots & \vdots & \ddots & \vdots \\ 0 & 0 & \cdots & 0 \end{pmatrix}.$$

When $\mathbf{H} = 0$, the recurrence phenomenon already exists in the first-order equation (4.8). To observe this, we introduce the following lemma:

Lemma 5. *For any $m > 0$, there exists a diagonal matrix \mathbf{D}_m such that such that the matrix*

$$\mathbf{D}_m \left(\mathbf{A} + \frac{1}{(mk)^2} \mathbf{G} \right) \mathbf{D}_m^{-1}$$

is symmetric and tridiagonal, and therefore the matrix $\mathbf{A} + (mk)^{-2} \mathbf{G}$ is real diagonalizable.

Proof. The matrix \mathbf{D}_m can be explicitly written as

$$(4.11) \quad \mathbf{D}_m = \text{diag} \left\{ 1, \frac{mk}{\sqrt{(mk)^2 + 1}}, \frac{mk}{\sqrt{(mk)^2 + 1}}, \dots, \frac{mk}{\sqrt{(mk)^2 + 1}} \right\}.$$

It can then be easily verified that

$$\mathbf{D}_m \left(\mathbf{A} + \frac{1}{(km)^2} \mathbf{G} \right) \mathbf{D}_m^{-1} = \begin{pmatrix} 0 & \sqrt{1 + (mk)^{-2}} & 0 & 0 & \cdots & 0 \\ \sqrt{1 + (mk)^{-2}} & 0 & \sqrt{2} & 0 & \cdots & 0 \\ 0 & \sqrt{2} & 0 & \sqrt{3} & \cdots & 0 \\ 0 & \ddots & \ddots & \ddots & \ddots & \vdots \\ \vdots & \ddots & 0 & \sqrt{M-1} & 0 & \sqrt{M} \\ 0 & \cdots & 0 & 0 & \sqrt{M} & 0 \end{pmatrix}.$$

□

The above lemma shows that when $\mathbf{H} = 0$, all the eigenvalues of $ik(\mathbf{A} + k^{-2} \mathbf{G})$ are purely imaginary, which indicates that $\hat{\mathbf{f}}^{(1)}$ does not decay as time increases. Consequently, the relation (4.7) shows that the electric energy will not decay, resulting in the recurrence in the simple discretization of velocity without using filters.

4.2. Suppression of recurrence. This section focuses on the effect of the filter. As in Section 3.2, we assume again that the filter matrix \mathbf{H} is a negative semidefinite diagonal matrix with its first diagonal entry being zero and last diagonal entry being nonzero. In this section, we are going to show an exponential decay of the solution, which suppresses the recurrence. In detail, we have the following theorem:

Theorem 4. *Let $\mathbf{f}(x, t)$ be the series (4.5) where $\hat{\mathbf{f}}^{(0)}(t) \equiv (1, 0, \dots, 0)^T$ and $\hat{\mathbf{f}}^{(m)}$ with $m \geq 1$ are solved from the equations (4.8)(4.9). There exist constants $C^{(3)}$ and $\lambda^{(1)}$ such that*

$$(4.12) \quad \left\| \mathbf{f}(\cdot, t) - \hat{\mathbf{f}}^{(0)} \right\|_2 \leq C^{(3)} (t^M + 1) \exp(-\lambda^{(1)} t),$$

if ϵ is sufficiently small.

Similar to the case of the advection equation, the decay rate $\lambda^{(1)}$ is associated with the eigenvalues of matrices appearing in the equations. The following lemma gives a precise definition of $\lambda^{(1)}$:

Lemma 6. For all $m \in \mathbb{Z} \setminus \{0\}$, define

$$(4.13) \quad \mathbf{G}_m := -imk \left(\mathbf{A} + \frac{1}{(mk)^2} \mathbf{G} \right) + \mathbf{H}.$$

Then there exists a uniform constant $\lambda^{(1)} > 0$, such that all the eigenvalues of \mathbf{G}_m have real parts less than $-\lambda^{(1)}$. Furthermore, there exists a constant $C^{(4)}$ such that

$$(4.14) \quad \|\exp(t\mathbf{G}_m)\|_2 \leq C^{(4)}(t^M + 1) \exp(-\lambda^{(1)}t), \quad \forall m \in \mathbb{Z} \setminus \{0\}.$$

Proof. Consider the matrix

$$(4.15) \quad \mathbf{D}_m \mathbf{G}_m \mathbf{D}_m^{-1} = -imk \left(\mathbf{D}_m \left(\mathbf{A} + \frac{1}{(mk)^2} \mathbf{G} \right) \mathbf{D}_m^{-1} \right) + \mathbf{H},$$

which has the same eigenvalues as \mathbf{G}_m . Due to Lemma 5, we see that the above matrix is symmetric and tridiagonal, and all its subdiagonal entries are nonzero. Thus, we can use the same strategy as in the proof of Theorem 1 to show that all the eigenvalues of (4.15) have negative real parts. Similarly, since

$$\lim_{m \rightarrow \infty} \mathbf{D}_m \left(\mathbf{A} + \frac{1}{(mk)^2} \mathbf{G} \right) \mathbf{D}_m^{-1} = \mathbf{A},$$

showing the existence of a uniform bound $\lambda^{(1)}$ is an analog of the proof of Theorem 2. The details are left to the readers.

To show the inequality (4.14), we first follow the proof of Corollary 1 to get

$$(4.16) \quad \|\exp(t\mathbf{D}_m \mathbf{G}_m \mathbf{D}_m^{-1})\|_2 \leq C^{(2)}(t^M + 1) \exp(-\lambda^{(1)}t), \quad \forall m \in \mathbb{Z} \setminus \{0\}.$$

where $C^{(2)}$ is determined in the same way as $C^{(1)}$ in Corollary 1 and Theorem 2. Hence,

$$\begin{aligned} \|\exp(t\mathbf{G}_m)\|_2 &\leq \|\mathbf{D}_m^{-1}\|_2 \|\exp(t\mathbf{D}_m \mathbf{G}_m \mathbf{D}_m^{-1})\|_2 \|\mathbf{D}_m\|_2 \\ &= \sqrt{1 + \frac{1}{(mk)^2}} \|\exp(t\mathbf{D}_m \mathbf{G}_m \mathbf{D}_m^{-1})\|_2 \leq \sqrt{1 + \frac{1}{k^2}} C^{(2)}(t^M + 1) \exp(-\lambda^{(1)}t). \end{aligned}$$

Thus (4.14) holds for $C^{(4)} = \sqrt{1 + k^{-2}} C^{(2)}$. \square

In the above lemma, the estimate (4.14) gives the basic form of the decay rate. To turn (4.14) into an estimate of the solution (4.12), we follow the steps below:

- (1) Show that each non-constant term in the series (4.5) decays exponentially.
- (2) Show the convergence of the series for small ϵ .

The first step is established by proving the following theorem:

Theorem 5. Let $\hat{\mathbf{f}}^{(m)}$, $m \geq 1$ be the solutions to the equations (4.8)(4.9). For each positive integer m , there exists a constant $K^{(m)}$ such that

$$(4.17) \quad \left\| \hat{\mathbf{f}}^{(m)}(t) \right\|_2 \leq K^{(m)}(t^M + 1) \exp(-\lambda^{(1)}t).$$

Proof. Note that the equation (4.8) is linear. Therefore we can take $m = 1$ in (4.14) to get

$$(4.18) \quad \left\| \hat{\mathbf{f}}^{(1)}(t) \right\|_2 = \left\| \exp(\mathbf{G}_1 t) \hat{\mathbf{f}}^{(1)}(0) \right\|_2 \leq C^{(4)}(t^M + 1) \exp(-\lambda^{(1)}t).$$

Thus (4.17) is proven for $m = 1$ by taking $K^{(1)} = C^{(4)}$.

For $m \geq 2$, we use induction and suppose that the inequality

$$(4.19) \quad \left\| \hat{\mathbf{f}}^{(j)}(t) \right\|_2 \leq K^{(j)}(t^M + 1) \exp(-\lambda^{(1)}t),$$

holds for all $j < m$. To estimate $\hat{\mathbf{f}}^{(m)}(t)$, we write the explicit solution of (4.9) as

$$(4.20) \quad \hat{\mathbf{f}}^{(m)}(t) = \int_0^t \exp((t-s)\mathbf{G}_m) \mathbf{p}_m(s) ds,$$

where we have used the definition

$$(4.21) \quad \mathbf{p}_m(t) := -\frac{i}{k} \sum_{l=1}^{m-1} \hat{f}_0^{(l)}(t) \mathbf{B} \hat{\mathbf{f}}^{(m-l)}(t)$$

for conciseness. Since $\|\mathbf{B}\|_2 = \sqrt{M}$, the vector \mathbf{p}_m can be bounded by

$$(4.22) \quad \begin{aligned} \|\mathbf{p}_m(t)\|_2 &= \left\| -\frac{i}{k} \sum_{l=1}^{m-1} \frac{1}{l} \hat{f}_0^{(l)}(t) \mathbf{B} \hat{\mathbf{f}}^{(m-l)}(t) \right\|_2 \leq \frac{\sqrt{M}}{k} \sum_{l=1}^{m-1} \frac{1}{l} \|\hat{\mathbf{f}}^{(l)}(t)\|_2 \|\hat{\mathbf{f}}^{(m-l)}(t)\|_2 \\ &\leq \frac{\sqrt{M}}{k} \sum_{l=1}^{m-1} \frac{1}{l} K^{(l)} K^{(m-l)} (t^M + 1)^2 \exp(-2\lambda^{(1)}t), \end{aligned}$$

where the last inequality is an application of the inductive hypothesis. Now we can take the norm on both sides of (4.20) and plug in the inequalities (4.14) and (4.22) to get

$$(4.23) \quad \begin{aligned} \|\hat{\mathbf{f}}^{(m)}(t)\|_2 &\leq \int_0^t \|\exp((t-s)\mathbf{G}_m)\|_2 \|\mathbf{p}_m(s)\|_2 ds \\ &\leq C^{(5)} \sum_{l=1}^{m-1} \frac{1}{l} K^{(l)} K^{(m-l)} (t^M + 1) \exp(-\lambda^{(1)}t), \end{aligned}$$

where

$$(4.24) \quad C^{(5)} = \frac{\sqrt{M}}{k} C^{(4)} \int_0^\infty (s^M + 1)^2 \exp(-\lambda^{(1)}s) ds.$$

The inequality (4.23) shows that (4.17) holds for

$$(4.25) \quad K^{(m)} = C^{(5)} \sum_{l=1}^{m-1} \frac{1}{l} K^{(l)} K^{(m-l)} = C^{(5)} \sum_{l=0}^{m-2} \frac{1}{l+1} K^{(l+1)} K^{(m-l-1)}.$$

Therefore for all positive integer m , the estimate (4.17) holds according to the principle of the mathematical induction. \square

From the above theorem, we see that if the distribution function (4.5) is approximated by a truncation of the series, then such a finite series converges to a constant as $t \rightarrow \infty$. To prove such a property for the infinite series (4.5), we still need to study the magnitude of each coefficient $K^{(m)}$. The recursion relation (4.25) reminds us of Jonah's theorem introduced in [17]:

Lemma 7 (Jonah). *If $m_1 \geq 2m_2$, then*

$$(4.26) \quad \binom{m_1 + 1}{m_2} = \sum_{l=0}^{m_2} \frac{1}{l+1} \binom{2l}{l} \binom{m_1 - 2l}{m_2 - l}.$$

By this lemma, a general formula of $K^{(m)}$ can be explicitly written, and then it can be properly bounded. The details are listed in the following proof:

Proof of Theorem 4. We first claim that

$$(4.27) \quad K^{(m+1)} = \frac{1}{2^m} \binom{2m}{m} K^{(1)} \left(C^{(5)} K^{(1)} \right)^m.$$

Apparently the above equality holds for $m = 0$. If $m > 0$, we just need to verify that (4.27) fulfills (4.25). By inserting (4.27) into (4.25) and cancelling out some constants on both sides, we obtain

$$(4.28) \quad \frac{1}{2} \binom{2m}{m} = \sum_{l=0}^{m-1} \frac{1}{l+1} \binom{2l}{l} \binom{2(m-l-1)}{m-l-1}.$$

To verify this equality, we apply Jonah's theorem (4.26) and let $m_1 = 2(m-1)$, $m_2 = m-1$. Thus the right hand side of (4.28) matches the right hand side of (4.26). The left hand sides are also equal since

$$(4.29) \quad \frac{1}{2} \binom{2m}{m} = \frac{1}{2} \frac{(2m)!}{m!m!} = \frac{1}{2} \frac{2m}{m} \frac{(2m-1)!}{m!(m-1)!} = \binom{2m-1}{m-1} = \binom{m_1+1}{m_2}.$$

Based on (4.27), it is easy to bound $K^{(m)}$ by

$$(4.30) \quad K^{(m+1)} = 2^m \frac{(2m-1)!!}{(2m)!!} K^{(1)} \left(C^{(5)} K^{(1)} \right)^m \leq K^{(1)} \left(2C^{(5)} K^{(1)} \right)^m.$$

Now we can use (4.5) to get

$$(4.31) \quad \begin{aligned} \left\| \mathbf{f}(\cdot, t) - \hat{\mathbf{f}}^{(0)} \right\|_2 &\leq \sqrt{D} \sum_{m=0}^{+\infty} \epsilon^{m+1} \left\| \hat{\mathbf{f}}^{(m+1)} \right\|_2 \leq \sqrt{D} \sum_{m=0}^{+\infty} \epsilon^{m+1} K^{(m+1)} (t^M + 1) \exp(-\lambda^{(1)} t) \\ &\leq \epsilon D K^{(1)} \sum_{m=0}^{+\infty} \left(2\epsilon C^{(5)} K^{(1)} \right)^m (t^M + 1) \exp(-\lambda^{(1)} t). \end{aligned}$$

Now it is clear that when $\epsilon < [2C^{(5)} K^{(1)}]^{-1}$, the inequality (4.12) holds for

$$(4.32) \quad C^{(3)} = \frac{\epsilon D K^{(1)}}{1 - 2\epsilon C^{(5)} K^{(1)}}. \quad \square$$

4.3. Analysis on the damping rate of the electric energy. In this section, we will analyze how the filter affects the damping rate and the oscillation frequency of the electric energy in the problem of Landau damping. Below we will first review the analysis on the original VP equation, and then the filtered equation will be discussed.

4.3.1. Analysis on the VP equation. In the linear Landau damping problem, the plasma wave has very small amplitude. Thus we can assume that

$$(4.33) \quad f(x, \xi, t) = f^{(0)}(\xi) + \epsilon f^{(1)}(x, \xi, t),$$

where $f^{(0)}(\xi)$ is the background distribution, which is uniform in x , and $f^{(1)}(x, \xi)$ has the order of magnitude $O(1)$. Inserting this equation into the VP equation and ignoring the terms quadratic in ϵ , we get the following linearized VP equation:

$$(4.34) \quad \frac{\partial f^{(1)}}{\partial t} + \xi \frac{\partial f^{(1)}}{\partial x} + E^{(1)} \frac{\partial f^{(0)}}{\partial \xi} = 0, \quad \frac{\partial E^{(1)}}{\partial x} = \int_{\mathbb{R}} f^{(1)} d\xi.$$

If we further assume that the plasma wave being considered takes the form of a plane wave traveling in the x -direction:

$$(4.35) \quad f^{(1)}(x, t, \xi) = \hat{f}^{(1)}(\xi) \exp(-i\omega t + ikx), \quad E^{(1)}(x, t) = \hat{E}^{(1)} \exp(-i\omega t + ikx),$$

we obtain the dispersion relation

$$(4.36) \quad \frac{1}{k^2} \int_{\mathbb{R}} \frac{1}{\xi - \omega/k} \frac{\partial f^{(0)}}{\partial \xi} d\xi = 1.$$

Let $\omega = \omega_p + i\gamma$ be the solution to (4.36). Then γ and ω_p are respectively the damping rate and the oscillation frequency of the electric energy. We refer the readers to [11] for the more details on the dispersion relation.

4.3.2. Analysis on the filtered VP equation. In order to take into account the filters, we assume that the filter (2.11) is used and consider the “modified equation” (2.12), so that a similar analysis can be carried out. Here we also assume that the distribution function is a small perturbation of the background distribution (4.33), and the linearized VP equation with filter can be written as

$$(4.37) \quad \frac{\partial f^{(1)}}{\partial t} + \xi \frac{\partial f^{(1)}}{\partial x} + E^{(1)} \frac{\partial f^{(0)}}{\partial \xi} = \mathcal{H}f^{(1)}, \quad \frac{\partial E^{(1)}}{\partial x} = \int_{\mathbb{R}} f^{(1)} d\xi,$$

where the operator \mathcal{H} is defined by $\mathcal{H} = (-1)^{p+1} \alpha (\Delta t M^p)^{-1} \mathcal{D}^p$, and we have assumed $\mathcal{H}f^{(0)} = 0$, which holds for the initial condition (4.3). Let

$$(4.38) \quad g(x, \xi, t) = \exp(-t\mathcal{H})f^{(1)}(x, \xi, t).$$

Then the function g formally satisfies

$$(4.39) \quad \exp(t\mathcal{H}) \frac{\partial g}{\partial t} = - \left(\xi \exp(t\mathcal{H}) \frac{\partial g}{\partial x} + E^{(1)} \frac{\partial f^{(0)}}{\partial \xi} \right), \quad \frac{\partial E^{(1)}}{\partial x} = \int_{\mathbb{R}} \exp(t\mathcal{H})g d\xi.$$

Now we assume that the equation (4.39) has a plane-wave solution:

$$(4.40) \quad g(x, \xi, t) = \hat{g}(\xi) \exp(-i\omega t + ikx), \quad E^{(1)}(x, t) = \hat{E}^{(1)} \exp(-i\omega t + ikx),$$

which changes (4.39) into

$$(4.41) \quad i(\xi k - \omega) \exp(t\mathcal{H})\hat{g} = -\hat{E}^{(1)} \frac{\partial f^{(0)}}{\partial \xi}, \quad ik\hat{E}^{(1)} = \int_{\mathbb{R}} \exp(t\mathcal{H})\hat{g} d\xi.$$

By dividing the first equation by $\xi k - \omega$ and integrating with respect to ξ , the amplitude of the electric field $\hat{E}^{(1)}$ can be cancelled out and we get the result

$$(4.42) \quad k = \int_{\mathbb{R}} \frac{1}{\xi k - \omega} \frac{\partial f^{(0)}}{\partial \xi} d\xi,$$

which turns out to be exactly the same as the result of the original VP equation (4.36). Such analysis shows that the modified equation and the original VP equation have the same damping rate and oscillation frequency for the electric field. Therefore adding filters does not ruin the major behavior of the linear Landau damping.

Remark 2. The above analysis is only formally correct, since in (4.38), the operator $\exp(-t\mathcal{H})$ is generally an unbounded operator. Therefore it still remains to prove that $f^{(1)}$ lies in the domain of this operator for all x and t , which is not yet done. Currently we are not too concerned about this point since the main idea of this section is to provide a clue for the reliability of filters.

5. NUMERICAL RESULTS

In order to verify the theoretical results and show how the recurrence is suppressed by the filter, the numerical experiments for both the advection equation and the Vlasov equation are carried out. In the literature, the recurrence for the Landau damping problem is usually observed from the evolution of the self-consistent electric energy $\mathcal{E}(t)$ defined in (4.4). Therefore in all the numerical tests, we are going to use the same quantity (4.4) to show the effect of the filter. Note that for the advection equations considered in Section 3, we do not have $E(x, t) = E_{sc}(x, t)$ as in the Vlasov equation, and thus the quantity $\mathcal{E}(t)$ is merely a functional of the distribution function $f(x, \xi, t)$ defined by (4.1) (4.4), and does not appear explicitly in the transport equation.

The filter we adopt in our numerical tests is the one proposed in [20], which is identical to the filter defined in (2.11) with $\alpha = 36$ and $p = 36$. The corresponding filter matrix \mathbf{H} can be written as (2.15) with

$$(5.1) \quad h_i = -36\Delta t^{-1}(i/M)^{36}, \quad i = 0, \dots, M.$$

As mentioned in Section 2, the time step Δt is set as $\Delta t = C/\sqrt{M}$, and the constant C is chosen as 0.5 in all the tests. Since it is much easier to obtain $\mathcal{E}(t)$ from the Fourier coefficients $\hat{\mathbf{f}}^{(m)}$, we solve (2.18) instead of the original transport equation (1.2) in all our experiments.

5.1. Advection equation. In this section, we focus on the advection equation (3.1) with initial condition (3.2). This initial condition gives the following Fourier coefficients:

$$\hat{\mathbf{f}}^{(0)}(0) = (1, 0, \dots, 0)^T, \quad \hat{\mathbf{f}}^{(-1)}(0) = \hat{\mathbf{f}}^{(1)}(0) = (\epsilon/2, 0, \dots, 0)^T, \quad \hat{\mathbf{f}}^{(m)}(t) = 0, \quad |m| \geq 2.$$

In this case, the equations (3.3) shows that each $\hat{\mathbf{f}}^{(m)}$ can be solved independently, and when $|m| \geq 2$, the initial condition shows that $\hat{\mathbf{f}}^{(m)}(t) \equiv 0$. Consequently, the function $\mathcal{E}(t)$ has a simple form

$$(5.2) \quad \mathcal{E}(t) = \sqrt{\frac{D}{k^2} \left(\left| \hat{f}_0^{(-1)}(t) \right|^2 + \left| \hat{f}_0^{(1)}(t) \right|^2 \right)}.$$

The exact solution of $\mathcal{E}(t)$ can be directly obtained from (3.7) as

$$(5.3) \quad \mathcal{E}(t) = \frac{\epsilon}{k} \sqrt{\frac{D}{2}} \exp(-k^2 t^2 / 2).$$

To obtain $\mathcal{E}(t)$ with the spectral method, we just need to apply (3.9) for $m = \pm 1$, which requires diagonalization of matrices $\mathbf{A}_{\pm 1}$.

In this example, we set $D = 4\pi$ and $k = 2\pi/D = 1/2$. We first verify that all the eigenvalues of $\mathbf{A}_{\pm 1}$ have negative real parts. Since $\mathbf{A}_1 = \mathbf{A}_{-1}^*$, the eigenvalues of \mathbf{A}_1 are the complex conjugates of those of \mathbf{A}_{-1} . Therefore it is sufficient to just look at \mathbf{A}_1 . The distribution of the eigenvalues of \mathbf{A}_1 on the complex plane is plotted in Figure 1, and the eigenvalues of $ik\mathbf{A}$ (the case without filter) are also given as a reference. As predicted, all the eigenvalues of $ik\mathbf{A}$ locate exactly on the imaginary axis, while all the eigenvalues of \mathbf{A}_1 have strictly negative real parts.

The time evolutions of \mathcal{E} and its logarithm are plotted respectively in Figure 2 and 3. Initially, both numerical solutions with and without the filter decay in the same way as the exact solution. When the evolution reaches the first ‘‘critical’’ point, almost simultaneously, both solutions leave the exact solution and exhibit a fast growth. For the case without filter, the value of $\mathcal{E}(t)$ bounces almost back to its initial value before the next decay, and such a process repeats periodically, which implies a constantly appearing recurrence. In general, larger number of

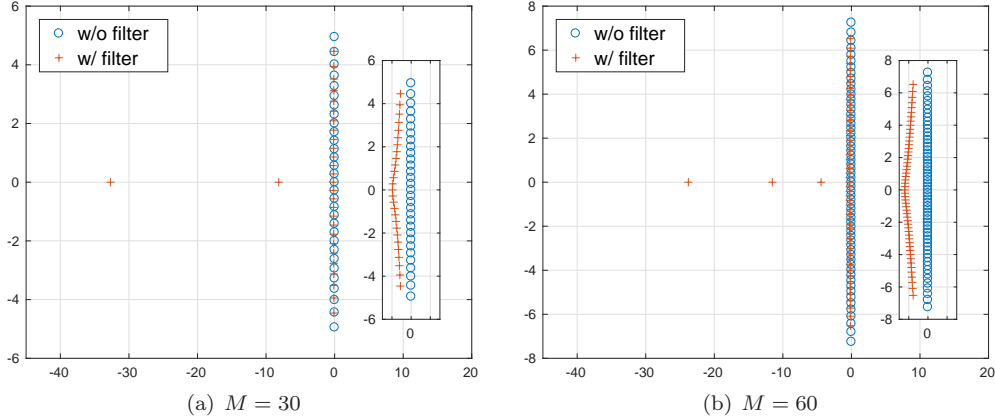


FIGURE 1. The eigenvalues of $ik\mathbf{A}$ and \mathbf{A}_1 with $M = 30$ and 60 . The circles are the eigenvalues of $ik\mathbf{A}$ and the plus signs are the eigenvalues of \mathbf{A}_1 .

moments leads to a longer recurrence time, which can also be observed by comparing the results with $M = 30$ and $M = 60$. When the filter is applied, the solutions behave similarly except that the peak values get smaller as t gets larger, due to the damping effect of the filter. It can also be observed that the damping rate for $M = 60$ is higher than that for $M = 30$, which indicates that for the same filter, systems with more moments may have better suppression of recurrence. We comment here that the recurrence is not completely eliminated since $\mathcal{E}(t)$ is still not monotonically decreasing. Nevertheless, from Figure 2, one sees that the difference between the numerical solution and the analytical solution is negligible when t is large.

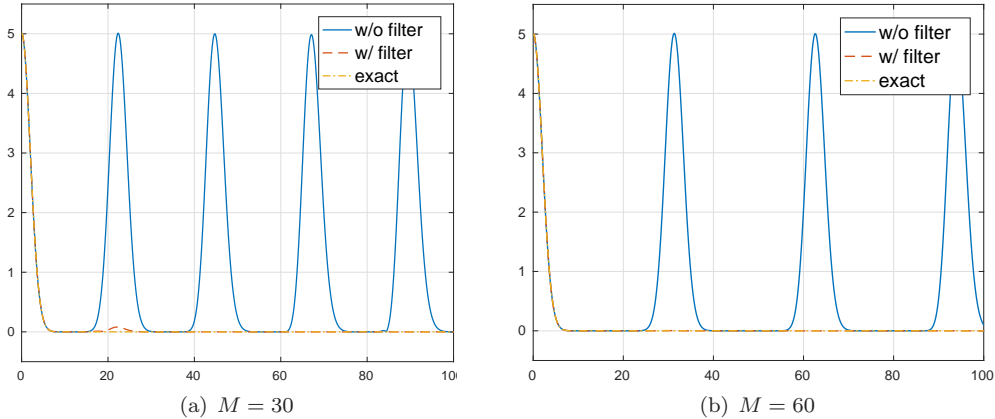
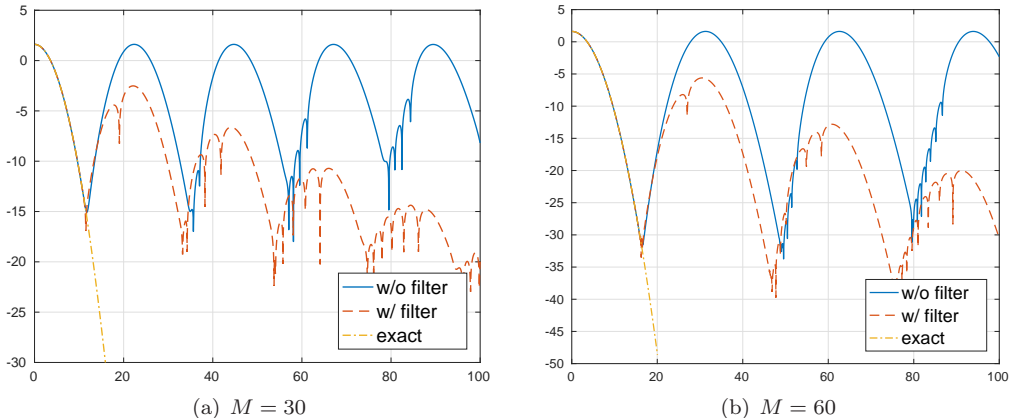
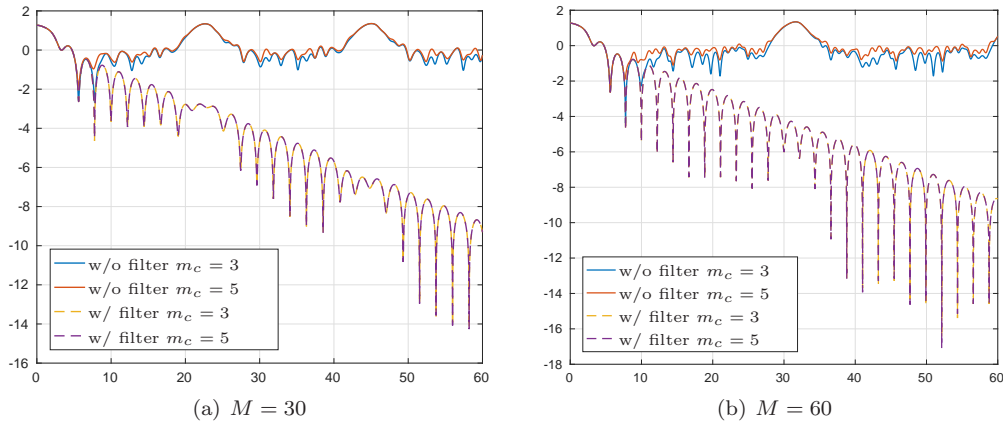


FIGURE 2. The time evolution of $\mathcal{E}(t)/\epsilon$ with $M = 30$ and 60 .

5.2. Advection equation with given force field. In this section, some numerical experiments for the transport equation with a given force field (3.21) are performed. Here we choose $\alpha(t)$ and $w(t)$ respectively as

$$(5.4) \quad \alpha(t) = \gamma t, \quad w(t) = \epsilon \cos(\omega t) \exp(ikx),$$


 FIGURE 3. The time evolution of $\log(\mathcal{E}(t)/\epsilon)$ with $M = 30$ and 60 .

 FIGURE 4. The evolution of $\log \mathcal{E}(t)$ for the example in Section 5.2.

so that it mimics the Landau damping process. The period and the wave number are again chosen as $D = 4\pi$, $k = 0.5$. For Landau damping, these parameters give the decay rate $\gamma = 0.15336$ and the plasma oscillation frequency $\omega = 1.416$ (see Section 5.3 for details), which are also adopted in definition of $w(t)$. The initial condition is given by (4.3). To see the contribution from waves with higher frequencies, we set ϵ to be 0.9. In order to carry out the numerical simulation, only Fourier modes with $|m| \leq m_c$ are taken into account.

Two numbers of moments $M = 30$ and $M = 60$ are simulated with $m_c = 3$ and $m_c = 5$. The time evolution of the logarithm of \mathcal{E} is plotted in Figure 4, which also shows clearly how the filter improves the solution. Figure 5 also shows such an effect from another point of view, where all the non-constant modes are taken into account. For the case with filters, the decay of each mode is given in Figure 6. A reference decay rate given by the largest real part of the eigenvalues of \mathbf{A}_m is also provided as a reference. It is seen that the decay rates of all the Fourier modes are controlled by this reference line.

5.3. Linear Landau damping. The numerical effect of the filter in the simulation of linear Landau damping has been studied in a number of previous works [23, 24]. Here some simple

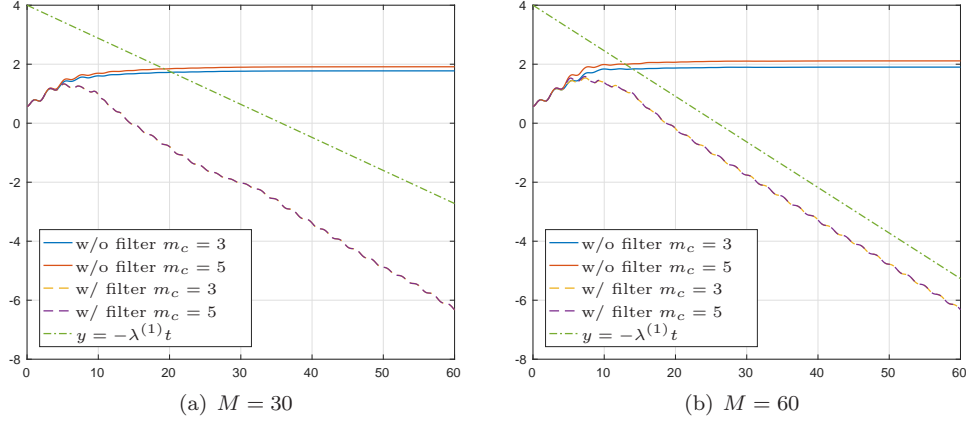


FIGURE 5. The evolution of $\log(\|\hat{\mathbf{f}} - \hat{\mathbf{f}}^{(0)}\|_2)$ for the example in Section 5.2.

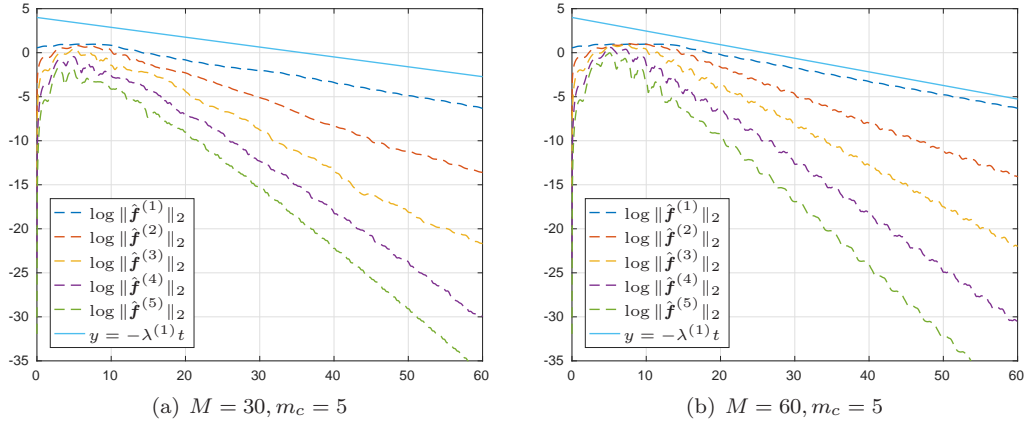


FIGURE 6. The evolution of $\log(\|\hat{\mathbf{f}}^{(m)}\|_2)$ for the example in Section 5.2.

results are presented for our particular discretization (2.1). The parameters are chosen as $\epsilon = 0.001$, $D = 4\pi$ and $k = 1/2$. Since ϵ is quite small, it is sufficient to consider the leading order term $\epsilon \hat{E}^{(1)}(t) \exp(ikx)$ in the expansion (4.6).

The evolution of $\log \mathcal{E}(t)$ with $M = 90$ and $M = 120$ is plotted in Figure 7, where the solutions with and without filters are both given. We can find that the two solutions are almost the same before the recurrence occurs. Similar to in the last subsection, after the recurrence time, the results without filters become unreliable, while the results with filters still decay exponentially. To be precise, the numerical decay rate is obtained by least-square fitting of peak value points before time t_F . Two different values of t_F (respectively before and after recurrence) are used to fit the slope, and the results are compared with the theoretical decay rate $\gamma = 0.15336$ (see e.g. [27]). Particularly, the second t_F is chosen around twice the recurrence time. Table 1 shows that before recurrence, the decay rates of both methods match very well with the theoretical result, and after the recurrence time, an accurate decay rate can still be kept for a long time

by filtering. In this example, the filter improves the numerical result dramatically, and such a method looks very promising in the numerical simulation of plasmas.

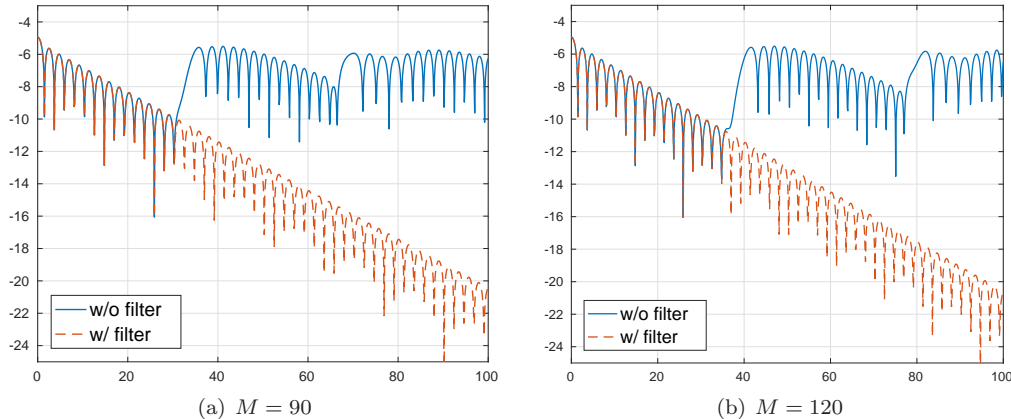


FIGURE 7. The evolution of $\log \mathcal{E}(t)$ for the Landau damping problem.

TABLE 1. The numerical decay rates of the electric energy

M	w/o filter	w/ filter	w/ filter	M	w/o filter	w/ filter	w/ filter
30	$t_F = 12$ 0.155038	$t_F = 12$ 0.1550545	$t_F = 24$ 0.200223	60	$t_F = 22$ 0.1540681	$t_F = 22$ 0.1540679	$t_F = 44$ 0.166939
90	$t_F = 26$ 0.154173	$t_F = 26$ 0.154173	$t_F = 52$ 0.152892	120	$t_F = 30$ 0.153780	$t_F = 30$ 0.153780	$t_F = 60$ 0.153629

6. CONCLUSION

In this paper, we have systematically analyzed the effect of the filter on the numerical solutions to the transport equations using Hermite-spectral method. The theoretical analysis on two types of transport equations is proposed respectively. It is both rigorously proven and numerically validated that the filter makes all the non-constant modes damp exponentially, and therefore suppresses the recurrence. The example of Landau damping shows that the filter has only negligible effect on the damping rates of the electric energy, which illustrates that adding filter is a promising method to relieve the recurrence phenomenon. Analysis on the case with magnetic field will be studied in the future.

REFERENCES

- [1] H. Abbasi, M. H. Jenab, and H. H. Pajouh. Preventing the recurrence effect in the Vlasov simulation by randomizing phase-point velocities in phase space. *Phys. Rev. E.*, 84(3):036702, 2011.
- [2] C. K. Birdsall and A. B. Langdon. *Plasma physics via computer simulation*. Institute of Physics Publishing, Bristol/Philadelphia, 1991.
- [3] Z. Cai, R. Li, and Y. Wang. Solving Vlasov equation using NRxx method. *SIAM J. Sci. Comput.*, 35(6):A2807–A2831, 2013.
- [4] E. Camporeale, G. L. Delzanno, B. K. Bergen, and J. D. Moulton. On the velocity space discretization for the Vlasov-Poisson system: Comparison between implicit Hermite spectral and Particle-in-Cell methods. *Comput. Phys. Commun.*, 198:47–58, 2016.

- [5] C. Z. Cheng and G. Knorr. The integration of the Vlasov equation in configuration space. *J. Comput. Phys.*, 22:330–351, 1976.
- [6] S. Dawson and M. F. Wheeler. Particle simulation of plasma. *Reviews of Modern Physics*, 55:403–447, 1983.
- [7] L. Einkemmer and A. Ostermann. A strategy to suppress recurrence in grid-based Vlasov solvers. *Eur. Phys. J. D.*, 68(7):197, 2014.
- [8] L. Einkemmer and A. Ostermann. Convergence analysis of a discontinuous Galerkin/Strang splitting approximation for the Vlasov–Poisson equations. *SIAM J. Numer. Anal.*, 52(2):757–778, 2014.
- [9] F. Filbet and E. Sonnendrücker. Comparison of Eulerian Vlasov solvers. *Comput. Phys. Comm.*, 150(3):247–266, 2003.
- [10] F. Filbet, E. Sonnendrücker, and P. Bertrand. Conservative numerical schemes for the Vlasov equation. *J. Comput. Phys.*, 172:166–187, 2001.
- [11] R. J. Goldston and P. H. Rutherford. *Introduction to plasma physics*. Institute of Physics Pub, 2016.
- [12] D. Gottlieb and J. S. Hesthaven. Spectral methods for hyperbolic problems. *J. Comput. Appl. Math.*, 128:83–131, 2001.
- [13] F. C. Grant and M. R. Feix. Fourier-Hermite solutions of the Vlasov equations in the linearized limit. *Phys. Fluids*, 10(4):696–702, 1967.
- [14] R. W. Hamming. *Introduction to applied numerical analysis*. Taylor & Francis/Hemisphere, 1989.
- [15] R. E. Heath, I. M. Gamba, P. J. Morrison, and C. Michler. A discontinuous Galerkin method for the Vlasov-Poisson system. *J. Comput. Phys.*, 231(4):1140–1174, 2012.
- [16] P. P. Hilscher, K. Imadera, J. Q. Li, and Y. Kishimoto. The effect of weak collisionality on damped modes and its contribution to linear mode coupling in gyrokinetic simulation. *Phys. Plasmas*, 20:082127, 2013.
- [17] P. Hilton and J. Pedersen. The Ballot problem and Catalan numbers. *Nieuw Archief voor Wiskunde*, 8(2):209–216, 1990.
- [18] R. W. Hockney and J. W. Eastwood. *Computer simulation using particles*. McGraw-Hill, New York, 1981.
- [19] J. P. Holloway. Spectral velocity discretizations for the Vlasov-Maxwell equations. *Transport. Theor. Stat.*, 25(1):1–32, 1996.
- [20] T. Hou and R. Li. Computing nearly singular solutions using pseudo-spectral methods. *J. Comput. Phys.*, 226(1):379–397, 2007.
- [21] B. Kågström. Bounds and perturbation bounds for the matrix exponential. *BIT Numer. Math.*, 17(1):39–57, 1977.
- [22] T. Nakamura and T. Yabe. Cubic interpolated propagation scheme for solving the hyper-dimensional Vlasov-Poisson equation in phase space. *Comput. Phys. Commun.*, 120:122–154, 1999.
- [23] J. T. Parker and P. J. Dellar. Fourier-Hermite spectral representation for the Vlasov-Poisson system in the weakly collisional limit. *J. Plasma Phys.*, 81(02):305810203, 2015.
- [24] O. Pezzi, E. Camporeale, and F. Valentini. Collisional effects on the numerical recurrence in Vlasov-Poisson simulation. *Phys. Plasmas*, 23:022103, 2016.
- [25] E. Pohn, M. Shoucri, and G. Kamelander. Eulerian Vlasov codes. *Comput. Phys. Comm.*, 166(2):81–93, 2005.
- [26] J. Qiu and C. Shu. Positivity preserving semi-Lagrangian discontinuous Galerkin formulation: Theoretical analysis and application to the Vlasov-Poisson system. *J. Comput. Phys.*, 230(23):8386 – 8409, 2011.
- [27] E. Sonnendrücker. Approximation numérique des équations de Vlasov-Maxwell. *Notes du cours de M2*, 2010.
- [28] E. Sonnendrücker, J. Roche, P. Bertrand, and A. Ghizzo. The semi-Lagrangian method for the numerical resolution of Vlasov equations. *J. Comput. Phys.*, 149(2):201–220, 1998.
- [29] J. H. Wilkinson. *The algebraic eigenvalue problem*. Clarendon, 1965.
- [30] T. Zhou, Y. Guo, and C. W. Shu. Numerical study on Landau damping. *Physica D*, 157(4):322–333, 2001.

(Zhenning Cai) DEPARTMENT OF MATHEMATICS, NATIONAL UNIVERSITY OF SINGAPORE, LEVEL 4, BLOCK S17, 10 LOWER KENT RIDGE ROAD, SINGAPORE 119076

E-mail address: matcz@nus.edu.sg

(Yanli Wang) SCHOOL OF MATHEMATICS SCIENCE, PEKING UNIVERSITY, BEIJING, CHINA, 100871

E-mail address: wylmath@pku.edu.cn